

The Regulatory Effect of the Kinase Inhibitor PD98059 on Autophagic Flux During Trypsinogen Activation in Pancreatic Acinar Cells

Wenchao Yao, BS, Defu Zhu, BS, Haifeng Lu, BS, Chao Liu, BS, Bei Sun, PhD, Weihui Zhang, PhD, and Dongbo Xue, PhD

Objectives: To study the role of kinase inhibitor PD98059 on autophagy flow in the process of trypsinogen activation in pancreatic acinar cell and its related mechanism.

Methods: In the present study, bioinformatics analysis was used to predict kinases and their most relevant inhibitor (PD98059) which participates in autophagy of acute pancreatitis (AP). The rat pancreatic acini AR42J cells were divided into 4 groups: control group, sodium taurocholate hydrate (TLC) group, PD98059 group, and TLC + PD group. Twenty-seven Sprague-Dawley rats were divided into 3 groups ($n = 9$), including control group, severe AP (SAP) group, and SAP + PD group. We detected trypsinogen activation, autophagic activation, lysosome pH, and cathepsin-L activity *in vivo* and *in vitro*.

Results: Results revealed trypsinogen activation was significantly inhibited in mitogen-activated protein kinase 1, JAK2, LYN, and their common inhibitor was PD98059. The trypsinogen activation, Beclin1, and light chain 3 II expressions were reduced, whereas the expressions of lysosomal-associated membrane protein 2, cathepsin L1, and cathepsin-L activity is upregulated after the PD98059 pretreatment, both *in vivo* and *in vitro*.

Conclusions: Lysosomal dysfunction blocked autophagy flux, accompanied by increasing pancreatic acinar cell autophagy in the process of trypsinogen activation. PD98059 inhibited AP occurrence and pancreatic injury via improving the blocked autophagic pathway and reducing trypsinogen activation.

Key Words: acute pancreatitis, kinase inhibitors, autophagy, trypsinogen activation

(*Pancreas* 2020;49: 290–299)

Acute pancreatitis (AP) is a common clinical inflammatory disease. Our knowledge of AP has been improved continuously over years of clinical practice and scientific research. However, to date, there is still no effective treatment for AP, and the mortality rate of AP is high. At present, AP remains a difficult-to-treat acute condition in clinical practice that may require abdominal surgery.

Recent studies show that a variety of diseases are associated with autophagic disorders. Autophagy dysfunction may occur in any aspect of the autophagic process, including reduced production of autophagosomes, obstructed fusion with lysosomes, and decreased proteolytic activity.¹ It was found in an AP model that a large number of vacuoles accumulated in pancreatic acinar cells, and the accumulation of large vacuoles was positively correlated with the expression of microtubule-associated protein light chain 3 II (LC3II). The finding suggests that these vacuoles are of autophagic origin. Some studies found that intracellular activation of trypsinogen in early AP occurred in these large vacuoles. However, the degradation efficiency of sirtuins was decreased, and P62 expression was increased, which indicate that autophagy becomes less efficient in AP. The integrity and degradative capability of lysosomes mainly depend on lysosomal-associated membrane protein (LAMP) 1 (LAMP1) and LAMP2.² Lysosomal-associated membrane proteins are transmembrane proteins necessary for protection of the cytoplasm and lysosomes against the activity of acid hydrolases and that regulate the fusion of lysosomes with other organelles, particularly autophagosomes. In addition, LAMPs regulate the proteolytic activity and endocytosis of lysosomes.³

The activation of trypsinogen in pancreatic acinar cells is an important indicator of AP. It has been shown that treatment with autophagy inhibitors or knockout of the autophagy-related 5 (ATG5) gene significantly reduced trypsin activity and greatly attenuated the severity of AP.⁴ However, fasting-induced physiological autophagy failed to induce the activation of trypsinogen.⁵ These findings indicate that the aberrant activation of trypsinogen in AP is caused by the autophagic dysfunction rather than autophagy itself.

A recent study has shown that the mitogen-activated protein kinase (MAPK) signaling pathway plays an important role in the pathogenesis of AP, and the MAPK/c-Jun N-terminal kinase pathway has a regulatory effect on autophagy. However, the specific underlying mechanisms remain unclear.⁶ Also, Martinez-Lopez et al⁷ found that the phosphorylation level of ERK regulated the expression of autophagy-related proteins and that the extent of ERK phosphorylation was closely related to the expression of LC3II, the specific underlying mechanisms remain unclear. All these studies indicate that some signaling pathways and kinases have certain regulatory effects on autophagy in AP, but their results are often fragmentary and isolated. Bioinformatics technology can filter out all the kinases and kinase inhibitors that ever been studied and participate in the regulation of autophagy in AP. Kinase inhibitors that have been demonstrated to do may also be identified to provide guiding significance for clinical use.

Therefore, the present study screened all kinases participate in autophagy of AP by integrating analysis with methods of bioinformatics, and found out their inhibitors—PD98059. Our study then examined the severity of AP and the expression of autophagy-related proteins in pancreatic acinar cells and tissues pretreated with PD98059 in an attempt to determine, at the cellular and organismal levels, whether PD98059 can ultimately inhibit the intracellular

From the Department of General Surgery, The First Affiliated Hospital of Harbin Medical University, Harbin, China.

Received for publication September 6, 2018; accepted December 23, 2019.

Address correspondence to: Dongbo Xue, PhD, Department of General Surgery, The First Affiliated Hospital of Harbin Medical University, 23 You Zheng Street, Harbin 150001, China (e-mail: dongbo_xue@126.com).

B.S. and W.Z. participated in the data curation. W.Y. and D.X. participated in the formal analysis. D.X. participated in the funding acquisition. W.Y., C.L., and H.L. participated in the investigation. D.Z. and H.L. participated in the supplementing experiments. W.Y., D.Z., and H.L. participated in writing the original draft. D.X. participated in the writing review and editing.

This study was supported by the National Natural Science Foundation of China (grants 81770634 and 81570581).

The authors declare no conflict of interest.

Supplemental digital contents are available for this article. Direct URL citations appear in the printed text and are provided in the HTML and PDF versions of this article on the journal's Web site (www.pancreasjournal.com).

Copyright © 2020 Wolters Kluwer Health, Inc. All rights reserved.

DOI: 10.1097/MPA.0000000000001490

activation of trypsinogen through interference with the blocked autophagic pathway and define the underlying mechanisms. In future studies, we intend to focus on PD98059 and further explore the feasibility of its use as a targeted therapeutic drug for AP.

MATERIALS AND METHODS

Materials

Roswell Park Memorial Institute (RPMI) 1640 medium, fetal bovine serum (FBS) (Gibco, Carlsbad, Calif), pancreatin (Sigma, St. Louis, Mo), PD98059 (Beyotime, Beijing, China), sodium taurocholate hydrate (TLC) (Sigma), mammalian cell total protein extraction kit (Beyotime, Beijing, China), bicinchoninic acid (BCA) Protein Assay Kit (Wanleibio, Shenyang, China), trypsinogen activation peptide (TAP) ELISA kit (USCN, Wuhan, China), L-arginine (Sangon, Shanghai, China), and protease inhibitor (Roche, Nashville, Tenn).

Preliminary Experiments

Text Mining of Candidate Kinases

(1) Text mining of kinases associated with AP: The list of protein kinases were collected from protein kinase database (<http://kinasource.co.uk/Database/substrates.html>) and were imported into ActivePerl 5.16.2 software (ActiveState, Vancouver, Canada) with “acute pancreatitis.” Then, we searched the literature and documents in Pubmed with the key words, “each kinase” and “acute pancreatitis.” Second, with manual screening, we found protein kinases which are related to AP. (2) Text mining of kinases associated with autophagy: Information of human protein kinases were collected from protein kinase database (<http://kinasource.co.uk/Database/substrates.html>). First, search the literature and documents in Pubmed with key words of “autophagy” and “name of each kinase” for the autophagy-associated kinases. Second, with manual screening, check whether those found documents are related to autophagy. Candidate kinases associated with autophagy in the pathogenesis of AP were those appeared both in the first and second results.

Screening Kinases Regulating Trypsinogen Activation

(1) The siRNA-lipoRNAiMAX mixture (Lipofectamine RNAiMAX Transfection Reagent Cat. No 13778-150; Gibco) was prepared and added to a culture well containing 800 μ L of culture medium with cells. After 4 to 6 hours of culture, the culture medium was replaced with fresh medium (containing FBS and antibodies against 2 surface markers), followed by continuous culturing for 48 hours. The candidate kinases from bioinformatics analysis above were divided into different groups and each was treated with TLC (200 μ M TLC, 40 minutes). (2) Examination of trypsinogen activation by flow cytometry: the cells were treated with trypsin and harvested. Approximately 1×10^6 cells were collected from each group and centrifuged at 1000 rpm for 5 minutes. The supernatants were discarded, and the cell pellets were washed twice with phosphate-buffered saline (PBS). After each wash, the cells were centrifuged at 1000 rpm for 5 minutes. Subsequently, the cells were resuspended in 200 μ L of BZipAR working solution and incubated for 60 minutes at RT in the dark. After centrifugation at 1000 rpm for 5 minutes, the cells were resuspended in PBS and examined by flow cytometry. The experimental data were collected using the CellQuest software (Becton-Dickinson, San Jose, Calif) and analyzed using the Flowing Software (Becton-Dickinson).

Text Mining of Candidate Kinase Inhibitors

The list of protein kinase inhibitors were collected from protein kinase inhibitor database (<http://www.selleckbio.com/servlet/DownloadServlet?fileName=Selleck-Kinase-Inhibitor-Library>).

xlsx) and were imported into ActivePerl software (ActiveState) with “candidate kinases.” Then, we searched the literature and documents in Pubmed with the key words, “each kinase inhibitor” and “each candidate kinases.” Second, a visualized network was drawn with the software, Cytoscape (version 2.6.3, Cytoscape Consortium, San Diego, Calif) to exhibit the correlations between protein kinases and kinase inhibitors.

Cell-Based and Animal Experiments

Cell Culture and Grouping

AR42J cells were cultured in 90% RPMI 1640 medium supplemented with 10% FBS. The cells were separated into the control group (AR42J cells cultured under normal conditions), the TLC group (cells treated with 200 μ M TLC for 40 minutes), the PD group (cells treated with 10 μ M PD98059 for 30 minutes), and the PD + TLC group (cells treated with 10 μ M PD98059 for 30 minutes, followed by treatment with 200 μ M TLC for 40 minutes).

Confocal Microscopy

The cells grown in confocal dishes were washed with PBS and fixed in 150 μ L of paraformaldehyde at room temperature (RT) for 15 minutes. The cells were washed again with PBS and then incubated with PBS containing 2% Tween-20 at RT for 10 minutes. After washing with PBS, the cells were incubated with the working solution of BZipAR (Rhodamine 110, bus-[N-CBZ-L-isoleucyl-L-prolyl-L-arginine amide], dihydrochloride) (Molecular Probes; Thermo Fisher Scientific, Waltham, Mass) dye for 60 minutes at RT in the dark. The cells were then washed with PBS and immediately examined by confocal fluorescence microscopy.

Flow Cytometry

The cells were digested and harvested. Approximately 1×10^6 cells were collected from each group and centrifuged at 1000 rpm for 5 minutes. The supernatants were discarded, and the cell pellets were washed twice with PBS. After each wash, the cells were centrifuged at 1000 rpm for 5 minutes. Subsequently, the cells were resuspended in 200 μ L of BZipAR working solution and incubated for 60 minutes at RT in the dark. After centrifugation at 1000 rpm for 5 minutes, the cells were resuspended in PBS and examined by flow cytometry. The experimental data were collected using the CellQuest software (Becton-Dickinson) and analyzed using the Flowing Software (Becton-Dickinson).

Determination of Intracellular pH

Normal AR42J cells and the cells isolated from pancreatic tissue were seeded into 96-well plates. After cultivation of the cells for 24 hours, the culture medium was replaced with a standard solution of EMS buffer, containing 10 μ M monensin (Selleck, Shanghai, China), 20 μ M nigericin (MedChemExpress, Monmouth Junction, NJ), and LysoSensor Yellow/Blue DND-160 fluorescent dye (Thermo Fisher Scientific, Shanghai, China). To generate a pH gradient spanning 2 pH units (pH 4.0, 4.5, 5.0, 5.5, and 6.0), the solutions were adjusted with HCl/NaOH. After incubation at RT for 30 minutes, the ratios of fluorescence intensities at 340 and 380 nm (F340/380) were determined using a multimode microplate reader, and a standard curve of fluorescence intensity ratios vs pH was plotted. Various groups of cells were seeded into 96-well plates. Regular culture medium was replaced with culture medium containing LysoSensor Yellow/Blue DND-160 dye. After incubation at RT for 30 minutes, the lysosomal pH was calculated based on the corresponding standard curve.

Western Blot Analysis

The cells were digested, collected and incubated with 1 mL of lysis buffer. The resulting protein lysates were quantified using the BCA assay, conventionally electrophoresed and transferred to nitrocellulose membranes. Primary antibody incubation was as follows: the primary antibodies included LAMP2 antioat polyclonal antibody (1:200, sc-8100; Santa Cruz Biotech, Dallas, Texas); cathepsin L (CTSL) antioat polyclonal antibody (CTSL1, 1:200, sc-6498; Santa Cruz Biotech); and β -actin (1:5000, YM3028; Immunoway, Plano, Texas). After blocking, the membranes were first incubated with primary antibodies and then incubated with horseradish peroxidase-conjugated rabbit antioat IgG (H + L) secondary antibody at RT for 40 minutes with gentle shaking. Subsequently, the membranes were washed and incubated with ECL (Cat No. WBKLS0500; Millipore, Danvers, Mass) Western blotting substrate for 3 to 5 minutes. To visualize the target proteins, immunoblots were exposed to x-ray films. The films were then developed and fixed.

Concentration and Activity of CTSL1 Protein

(1) Measurement of protein concentration: The standard curve was created using bovine serum albumin (BSA) with a known concentration. Specifically, 0, 1, 2, 4, 8, 12, 16, and 20 μ L of BSA standard solution were added to different wells of a microtiter plate. Then each well was overlaid with 200 μ L of BCA working solution and incubated at 37°C for 20 minutes. The absorbance value at a wavelength of 570 nm was measured using a microplate reader. The protein concentrations of the samples were calculated based on the standard curve. (2) Examination of CTSL activity: Each sample well was loaded with 50 μ L of sample, each blank control well was loaded with 50 μ L of sample from the control group, while each negative control well was loaded with 50 μ L of cell lysis (CL) buffer. Subsequently, 50 μ L of CL buffer was added to each well, which was followed by addition of 1 μ L of dithiothreitol (DTT). The sample wells were then mixed with 2 μ L of 10 nM Ac-FR-7-amino-4-trifluoromethylcoumarin substrate; the blank and negative control wells were mixed with 2 μ L of cathepsin L inhibitor. After incubation at 37°C for 2 hours in the dark, the release of 7-amino-4-trifluoromethylcoumarin was measured using a multifunctional microplate reader at ex400 nm/em505 nm.

Construction of Animal Model and Grouping of the Animals

Twenty-seven healthy male Sprague-Dawley rats weighing 250 to 300 g each were subjected to adaptive feeding for 1 week. The rats were randomly divided into a sham-operated (control) group, the SAP group and the drug-treated (SAP + PD) group. The rats were fasted for 12 hours before each experiment. During the fasting period, the rats were allowed free access to water. At 1 hour before construction of the model, the SAP + PD group was given 4 mg/kg PD98059 via tail vein injection. Rats in the SAP group and the SAP + PD group received intraperitoneal injections of L-arginine (100 mg/100 g of body weight) twice at 1-hour intervals. Rats in the control group were injected with an equal volume of normal saline. At 24 hours after establishment of the model, blood was collected from all groups of rats, and serum was retained. Subsequently, the rats were killed, and the pancreatic tissues were harvested. Pancreatic tissues about the size of rice grains were prepared and fixed in 2.5% glutaraldehyde. A portion of the pancreas was fixed in 4% paraformaldehyde solution. The rest of the pancreatic tissues were rapidly frozen in liquid nitrogen and stored in a freezer at -70°C for future assays.

Hematoxylin-Eosin Staining

Pancreatic tissues were embedded and sectioned. The sections were dewaxed, rehydrated, stained, dehydrated, cleared, mounted, and microscopically examined. Images were taken at 200 \times magnification.

Determination of α -Amylase and TAP Activities

(1) The activity of α -amylase (AMS) was measured using the AMS Assay Kit (Gaochem, Shanghai, China) according to the manufacturer's instructions.

AMS activity in serum (U/dL) = (optical density [OD] value of the blank tube - measured OD value)/OD value of the blank tube \times 80

(2) Tissue protein samples were diluted to 5 μ g/ μ L with PBS. Sample loading: standard wells and sample wells were prepared. The standard wells (a total of 5 wells) were filled with various concentrations of the standard (50 μ L in each well), while the sample wells were filled with 50 μ L of samples for analysis. Immediately after loading the standards and samples, 50 μ L of test solution A was added to each well and mixed thoroughly by gentle shaking. The microtiter plates were then covered with parafilm and incubated at 37°C for 1 hour. After incubation, the liquid was discarded. The wells were washed by soaking for 2 minutes. Liquids in the microtiter plates were aspirated, and the wells were washed 3 times. Subsequently, 50 μ L of test solution B was added to each well of the microtiter plates. The plates were then covered with parafilm and incubated at 37°C for 30 minutes. After incubation, the liquids were aspirated from the wells. The plates were shaken dry and then washed 5 times. Afterward, 90 μ L of substrate solution was added to each well of the microtiter plates. The plates were then covered with parafilm and incubated at 37°C in the dark to allow color development. The chromogenic reaction was terminated by addition of 50 μ L of stop solution to each well. The OD value of each well was measured at a 450-nm wavelength using a microplate reader.

Statistical Methods

All experimental data were analyzed using GraphPad Prism 6.0 software (La Jolla, Calif). All data were presented as mean (standard deviation [SD]). Differences between the groups were analyzed using 1-way analysis of variance (ANOVA). A *P* value less than 0.05 indicated that the difference was statistically significant.

RESULTS

Preliminary Experiments

Text Mining of Candidate Kinases

In total, 28 kinases were obtained through text mining of "acute pancreatitis" and "the name of each kinase" and 62 kinases were obtained through text mining of "autophagy" and "the name of each kinase" in PubMed.

Ultimately, 9 candidate kinases associated with autophagy in the pathogenesis of AP were obtained from the intersection of them (Supplemental Fig. 1, <http://links.lww.com/MPA/A771>).

Screening Kinases Regulating Trypsinogen Activation

Flow cytometry results showed that silencing the kinases AKT, PKD1, EGFR, SRC, ROS, and MET did not significantly inhibit trypsinogen activation (*P* > 0.05). However, MAPK1, JAK2, and LYN did significantly inhibit trypsinogen activation (Supplemental Fig. 2, <http://links.lww.com/MPA/A771>).

Text Mining of Candidate Kinase Inhibitors

According to the kinases-kinase inhibitors network, PD98059 has regulatory effects on all of MAPK1, JAK2 and LYN, so PD98059 was selected as the candidate kinase inhibitor for subsequent studies. The results are shown in Figure 1.

Results of Cell-Based Experiments

Analysis of Trypsinogen Activation Results

Confocal laser scanning microscopy revealed that the fluorescence intensity was significantly increased in the TLC group compared with the control group. This finding indicated that trypsin activation was enhanced in the TLC group. In contrast, no significant difference was detected in the fluorescence intensity between the PD group and the control group. The fluorescence intensity was markedly reduced in the TLC + PD group compared with the TLC group. The results are shown in Figure 2A.

As shown in Figure 2B and C, quantitative flow cytometric analysis revealed that trypsinogen activation was significantly increased in AR42J cells after treatment with TLC ($P < 0.05$). Compared with the TLC group, cotreatment of AR42J cells with TLC and PD98059 resulted in markedly reduced trypsinogen activation ($P < 0.05$). The results indicated that PD98059 exerted an inhibitory effect on trypsinogen activation in AR42J cells. In consideration of the concentrations of the inhibitor applied blocks MAPK activity, we made a series of experiments. The results showed no significant effects between the control group and PD98059 groups in different concentrations (Supplementary Fig. 3, <http://links.lww.com/MPA/A771>).

Western Blot Analysis of the Expressions of Beclin 1, LC3, LAMP2, and CTSL1 in AR42J Cells

The effects of PD98059 on Beclin1 and LC3 proteins in AR42J cells: the expression of Beclin1 and LC3 were significantly

increased in the TLC group compared with the control group ($P < 0.05$). No significant difference was detected in the expression of Beclin1 and LC3 between the PD group and the control group ($P < 0.05$). The expression of Beclin1 and LC3 was markedly reduced in the TLC + PD group compared with the TLC group. The results are shown in Figure 3.

The effects of PD98059 on LAMP2 and CTSL1 proteins in AR42J cells: the expression of LAMP2 and CTSL1 was significantly decreased in the TLC group compared with the control group ($P < 0.05$). No significant difference was detected in the expression of LAMP2 and CTSL1 between the PD group and the control group ($P < 0.05$). The expression of LAMP2 and CTSL1 was significantly increased in the TLC + PD group compared with the TLC group. The results are shown in Figure 4. No significant difference was detected in the expression of pro-catL between the PD group and the control group, also between the TLC + PD group and TLC group ($P < 0.05$) (Supplementary Fig. 4, <http://links.lww.com/MPA/A771>).

Examination of the Activity of CTSL1 and catB Protein

The effects of PD98059 on the activity of CTSL1 and catB protein in AR42J cells: the activity of CTSL1 and catB protein was significantly decreased in the TLC group compared with the control group ($P < 0.05$). No significant difference was detected in the activity of CTSL1 and catB protein between the PD group and the control group ($P < 0.05$). The activity of CTSL1 protein was significantly increased, whereas the activity of catB was significantly decreased in the TLC + PD group compared with the TLC group. The results are shown in Figure 5.

Determination of Lysosomal pH

The lysosomal pH in each group was determined by the multifunction enzyme marker, and the results were calculated based

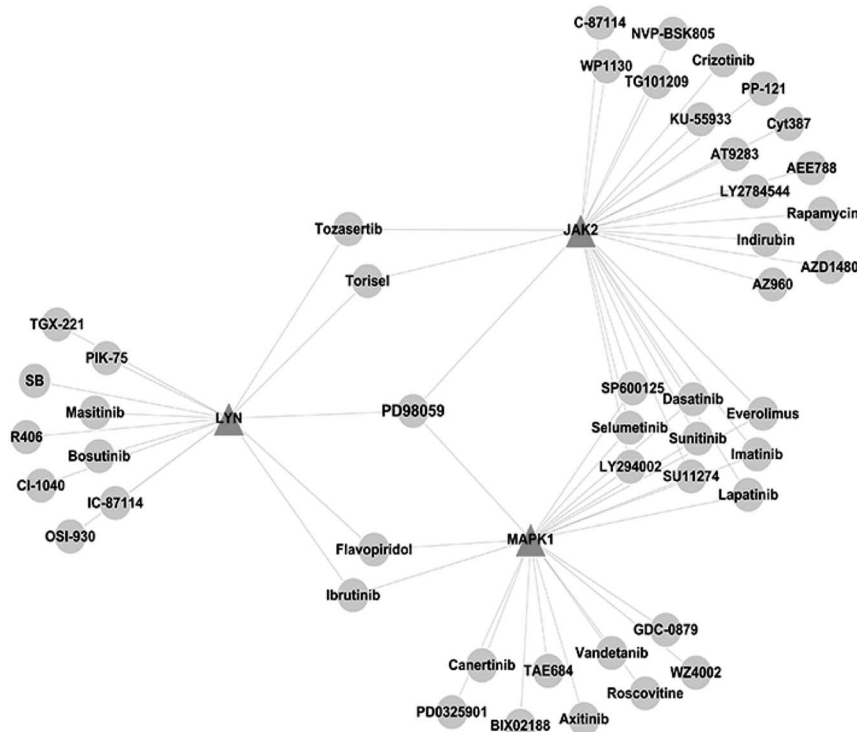


FIGURE 1. Network of kinase—kinase inhibitors of 3 candidate kinase candidates, MAPK1, JAK2, and LYN.

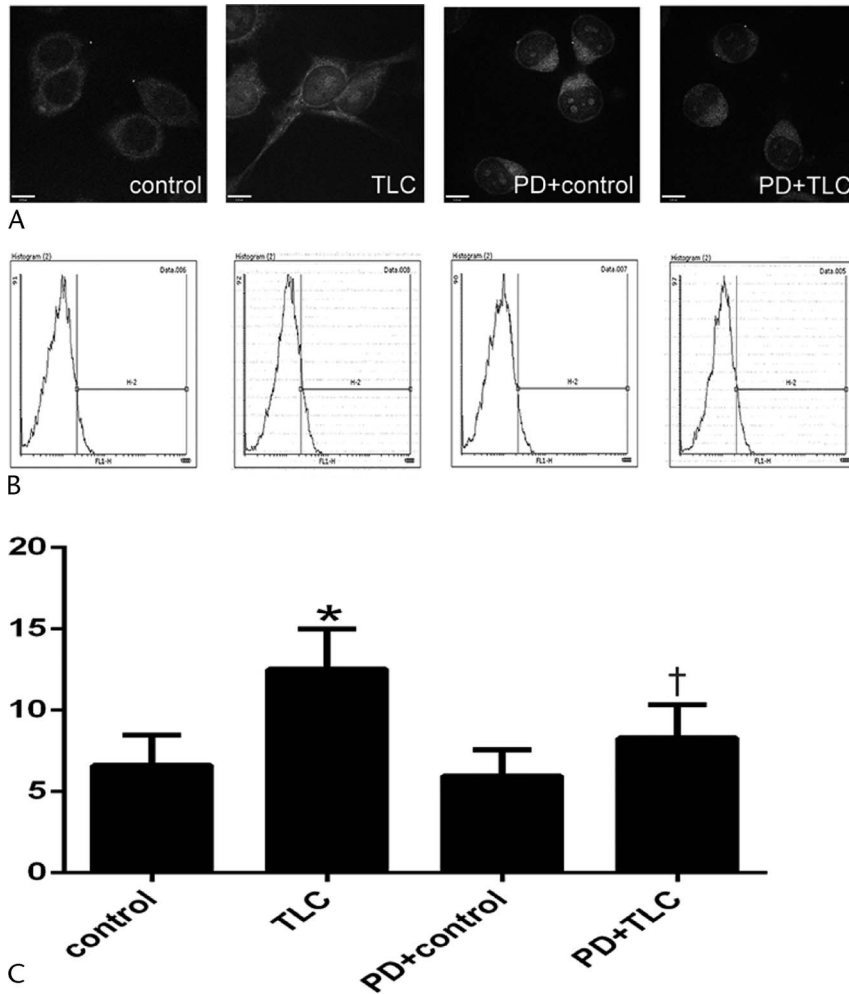


FIGURE 2. Acinar cell fluorescence intensity change and trypsinogen activation degree of detection. A, Image from laser confocal microscopy. B, Histogram of flow cytometry. C, Chart of statistics. *Compared with the control group, $P < 0.05$. †Compared with the TLC group, $P < 0.05$.

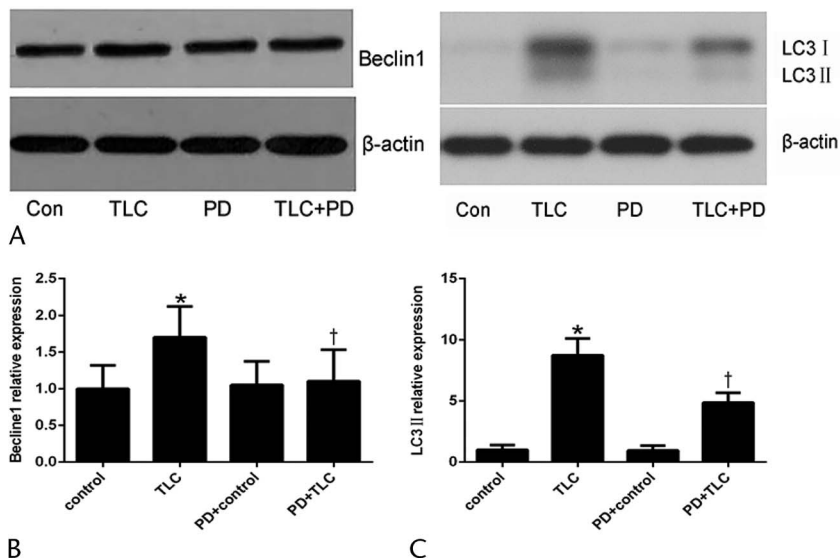


FIGURE 3. Western blot results for the Beclin1 and LC3 proteins expression in AR42J cells. A, Electrophoresis. B, Statistics chart of Beclin1 expression. C, Statistics chart of LC3 expression. *Compared with the control (Con) group, $P < 0.05$. †Compared with the TLC group, $P < 0.05$.

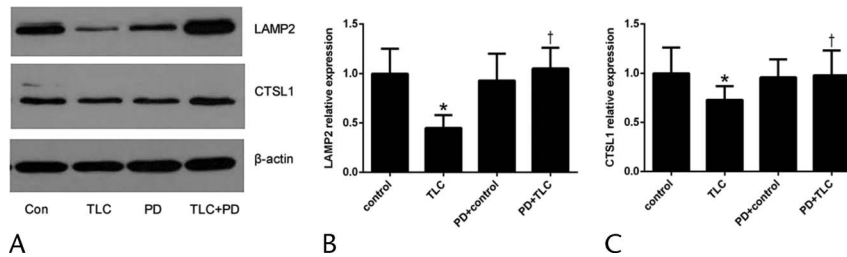


FIGURE 4. Western blot results for the LAMP2 and CTSL1 proteins expression in AR42J cells. A, Electrophoresis. B, Statistics chart of LAMP2 expression. C, Statistics chart of CTSL1 expression. *Compared with the control (Con) group, $P < 0.05$. †Compared with the TLC group, $P < 0.05$.

on the corresponding standard curve. The results revealed that the lysosomal pH was significantly increased in the TLC group compared with the control group ($P < 0.05$). This finding indicated that there was lysosomal dysfunction in the TLC group. No significant difference was detected in the lysosomal pH between the TLC + PD group and the TLC group ($P < 0.05$). This finding indicated that lysosomal function did not recover in the TLC + PD group. The results are shown in Supplementary Figure 5, <http://links.lww.com/MPA/A771>.

Results of Animal Experiments

Histopathologic Examination and Scoring

At 24 hours after the procedure, no necrotic cell death was observed in the pancreatic tissues of the rats in the control group. Only a portion of the pancreatic acinar cells in the control group exhibited edematous swelling. In addition, the control group exhibited clear lobular and interstitial structures in the pancreas, and there were no apparent signs of inflammatory cell infiltration in the pancreatic interstitium. In the SAP group, pancreatic acinar cells swelled significantly 24 hours after the procedure. Moreover, the acinar cells underwent necrosis in patches, which was accompanied by infiltration of many inflammatory cells. A disordered lobular structure, filled with a large amount of inflammatory exudates, was observed in the pancreas. In addition, microvessel ruptures occurred in the pancreatic interstitium in the SAP group, which was reflected by the release of many red blood cells. In the SAP + PD group, the pancreatic acinar cells displayed significant swelling at 24 hours after the procedure. However, no necrotic cell death was observed. There was infiltration of inflammatory cells among the acinar cells. In addition, interstitial edema was clearly visible, and inflammatory exudates were present between pancreatic lobules. The interlobular space was slightly widened. Very few microvessels were ruptured, and red blood cells were released. The results are shown in Supplementary Figure 6A, <http://links.lww.com/MPA/A771>.

All 3 groups of rats were examined under a microscope 24 hours after the procedure, and the pathological scores were as follows: control group, 1.80 (SD, 0.42); SAP group, 11.68 (SD, 1.28); and SAP + PD group, 15.93 (SD, 1.25). Both the SAP group and the SAP + PD group scored significantly higher than the control group ($P < 0.05$). Compared with the SAP group, the SAP + PD group had a significantly lower pathological score ($P < 0.05$). The results are shown in Supplementary Figure 6B, <http://links.lww.com/MPA/A771>.

Determination of AMS and TAP Activity

The activity of AMS was measured at 24 hours after the procedure, and the results were as follows: control group, 10.71 U/L (SD, 0.28 U/L); SAP group, 48.02 U/L (SD, 2.84 U/L); and SAP + PD group, 25.46 U/L (SD, 1.13 U/L). Both the SAP group and the SAP + PD group scored significantly higher than the control group ($P < 0.05$). Compared with the SAP group, the SAP + PD group had a significantly lower activity ($P < 0.05$). The results are shown in Supplementary Figure 7A, <http://links.lww.com/MPA/A771>.

The activity of TAP was measured at 24 hours after the procedure, and the results were as follows: control group, 90.78 pg/mL (SD, 3.52 pg/mL); SAP group, 390.01 pg/mL (SD, 5.57 pg/mL); and SAP + PD group, 164.95 pg/mL (SD, 3.89 pg/mL). Both the SAP group and the SAP + PD group scored significantly higher than the control group ($P < 0.05$). Compared with the SAP group, the SAP + PD group had a significantly lower activity ($P < 0.05$). The results are shown in Supplementary Figure 7B, <http://links.lww.com/MPA/A771>.

Western Blot Analysis of the Expressions of Beclin 1, LC3, LAMP2, and CTSL1 in Pancreatic Tissues

The effects of PD98059 on Beclin1 and LC3 proteins in the pancreatic tissues of the rats: the expression of Beclin1 and LC3 were significantly increased in the SAP group compared with the control group ($P < 0.05$). No significant difference was detected

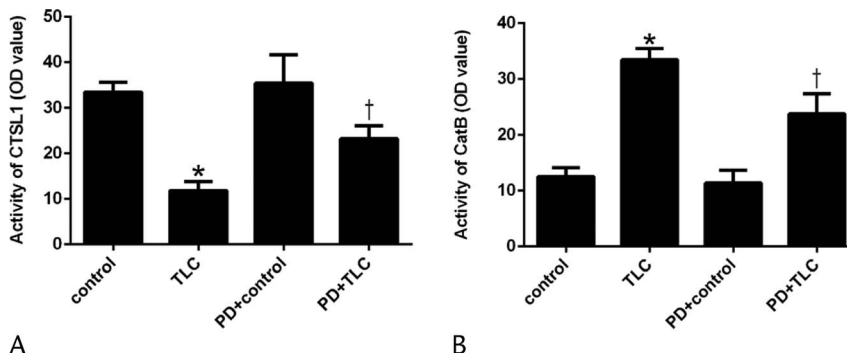


FIGURE 5. The activity of CTSL1 (A) and catB (B). *Compared with the control group, $P < 0.05$. †Compared with the TLC group, $P < 0.05$.

in the expression of Beclin1 and LC3 between the SAP + PD group and the control group ($P < 0.05$). The expression of Beclin1 and LC3 was markedly reduced in the SAP + PD group compared with the SAP group. The results are shown in Figure 6.

The effects of PD98059 on LAMP2 and CTSL1 proteins in the pancreatic tissues of the rats: the expression of LAMP2 and CTSL1 were significantly decreased in the SAP group compared with the control group ($P < 0.05$). No significant difference was detected in the expression of LAMP2 and CTSL1 between the SAP + PD group and the control group ($P < 0.05$). The expression of LAMP2 and CTSL1 was significantly increased in the SAP + PD group compared with the SAP group. The results are shown in Figure 7.

Examination of the Activity of CTSL1 and catB Protein

The effects of PD98059 on the activity of CTSL1 and catB protein in the pancreatic tissues of the rats: the activity of CTSL1 and catB protein was significantly decreased in the SAP group compared with the control group ($P < 0.05$). The activity of CTSL1 protein was significantly increased, whereas the activity of catB was significantly decreased in the SAP + PD group compared with the SAP group. The results are shown in Figure 8.

Determination of Lysosomal pH

The effects of lysosomal pH in the pancreatic tissues of the rats: the lysosomal pH were significantly increased in the SAP group compared with the control group ($P < 0.05$). No significant difference was detected in the lysosomal pH between the SAP + PD group and control group ($P < 0.05$). The lysosomal pH was significantly decreased in SAP + PD group compared with the SAP group. The results are shown in Supplementary Figure 8, <http://links.lww.com/MPA/A771>.

DISCUSSION

In the past decade, significant progress has been made in understanding the pathogenesis of AP. Aberrant activation of trypsinogen in pancreatic acinar cells is considered a key factor in

the occurrence of AP. However, the molecular mechanisms underlying the intracellular activation of trypsinogen remain unclear. Recent studies have found that autophagy may play a crucial role in the activation of trypsinogen. In the initial stage of AP, autophagy and aberrant activation of trypsinogen occur simultaneously. Moreover, early trypsinogen activation occurs in autophagic vacuoles of acinar cells.

In our study, we used the method of bioinformatics to select all of protein kinases involved in the regulation of autophagy in AP from protein kinase database. We made cell transfection and flow cytometry to validate their significant regulating meanings. In the same way, we screened out common kinase inhibitor (PD98059) of MAPK1, JAK2, LYN. It was also pointed out that PD98059 as a kinase inhibitor which can regulate the autophagy of AP.

At present, it is recognized that the abnormal activation of trypsinogen in pancreatic acinar cells is one of the major pathogenic factors for all types of AP. The degree of trypsinogen activation is an important indicator of the severity of AP. The present study examined the activation of trypsinogen in AR42J cells. It was found that trypsinogen activation was noticeably increased in both the TLC group and the TLC + PD group. However, the extent of the increase was significantly smaller in the TLC + PD group than that in the TLC group. The above findings indicate that PD98059 exerted an inhibitory effect on the activation of trypsinogen in pancreatic acinar cells. Therefore, PD98059 has a protective effect against the occurrence of AP. In addition, it is noteworthy that the TLC + PD group exhibited a significantly higher degree of trypsinogen activation in comparison to the control and PD groups ($P < 0.05$). This finding indicates that PD98059 only reduced the extent of trypsinogen activation but failed to completely block the aberrant intracellular activation of trypsinogen. The study also showed that PD98059 intervention alleviated the severity of inflammation in AP but failed to eliminate the inflammation.⁸ The findings are consistent with the results of the present study.

Autophagy is a dynamic process. The overall process of autophagy is referred to as autophagic flux, which includes the formation of autophagosomes, the transport of autophagic substrates

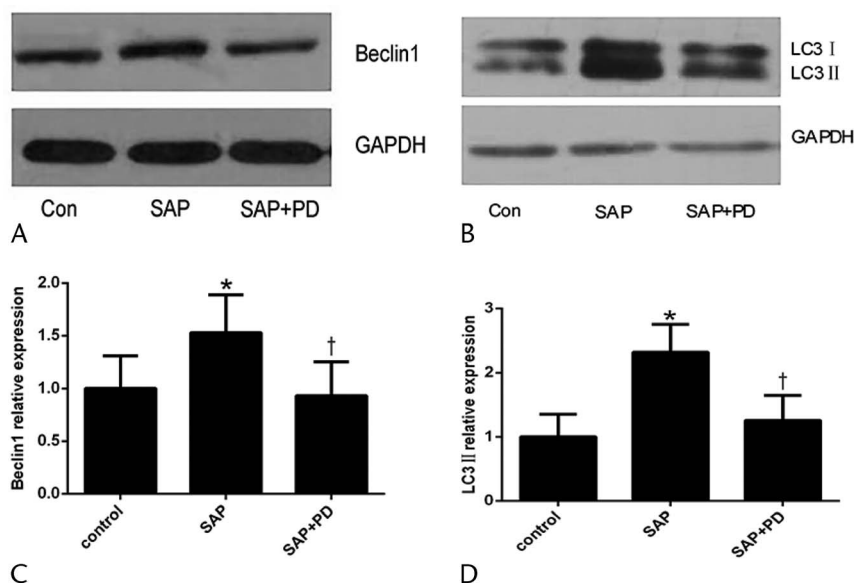


FIGURE 6. Western blot results for the Beclin1 and LC3 proteins expression in pancreatic tissue. A, Electrophoresis of Beclin1. B, Electrophoresis of LC3. C, Statistics chart of Beclin1 expression. D, Statistics chart of LC3 expression. *Compared with the control (Con) group, $P < 0.05$. †Compared with the SAP group, $P < 0.05$.

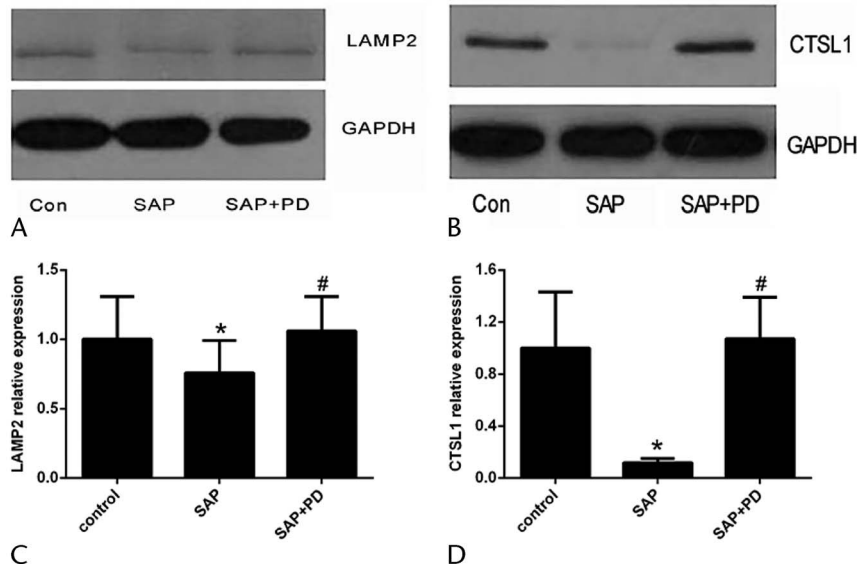


FIGURE 7. Western blot results for the LAMP2 and CTSL1 proteins expression in pancreatic tissue. A, Electrophoresis of LAMP2. B, Electrophoresis of CTSL1. C, Statistics chart of LAMP2 expression. D, Statistics chart of CTSL1 expression. *Compared with the control (Con) group, $P < 0.05$. †Compared with the SAP group, $P < 0.05$.

to lysosomes and the degradation of autophagic substrates in lysosomes. A simplified molecular mechanism is shown in Supplementary Figure 9, <http://links.lww.com/MPA/A771>.⁹

As a specific protein involved in autophagy in mammals, Beclin 1 plays an important role in the formation of autophagosome precursors and autophagosomal membranes.¹⁰ As shown in Supplementary Figure 9, <http://links.lww.com/MPA/A771>, LC3II is the most common marker on autophagosomal membranes.¹¹ In a cerulein-induced AP model, large vacuoles were formed and accumulated in the pancreatic acinar cells. Compared with starvation-induced vacuoles, the AP-related vacuoles were more numerous and larger in size. In pancreatic tissues, the increase in Beclin 1 and LC3II expression is consistent with the changes in the large vacuoles, which further confirmed the involvement of autophagy in the formation of autophagic vacuoles in acinar cells.¹² Moreover, the expressions of LC3II and Beclin 1 is upregulated in AP, and the extent of increase in LC3II and Beclin 1 expression is consistent with the severity of AP. The present study found that the expression of Beclin 1 and LC3II was downregulated in AR42J cells pretreated with PD98059. This finding indicates that the number of autophagosomes was significantly lower in the PD98059-pretreated acinar cells compared with the TLC group. However, the level of autophagic activity did not depend only on the number of autophagosomes. In fact, the autophagic activity level was proportional

to the degradation rate of autolysosomes. Autophagic activity was related to the activity of the autophagic pathway and autophagic flux. Unlike the physiological autophagy induced by starvation, the degradation efficiency of sirtuins was significantly reduced, and the expression level of P62 was elevated in the AP model, suggesting that autophagy was inefficient and that the autophagic pathway was blocked.¹³ In addition, animal experiments showed that Beclin 1 and LC3II levels were significantly lower in the SAP + PD group than in the SAP group and that the severity of pancreatic tissue injury was significantly reduced in the SAP + PD group. The above results demonstrate that PD98059 releases the blockage of the autophagic pathway in pancreatic acinar cells and enhances autophagy activity, thereby reducing the massive accumulation of autophagosomes and inhibiting the activation of trypsinogen. However, the specific mechanism by which PD98059 acts on autophagic flux remains to be elucidated.

In the early stages of AP, trypsinogen is transported into lysosomes via the formation of autophagosomes and autolysosomes. In lysosomes, trypsinogen is activated by cathepsin, forming trypsin, which then exerts a destructive effect.¹⁴ Lysosomal dysfunction is commonly observed in AP models. Lysosomal dysfunction-induced blockage of the autophagic pathway may be one of the major initiating factors for a series of pathophysiological changes in AP, including the intracellular activation of trypsinogen. The 2 notable

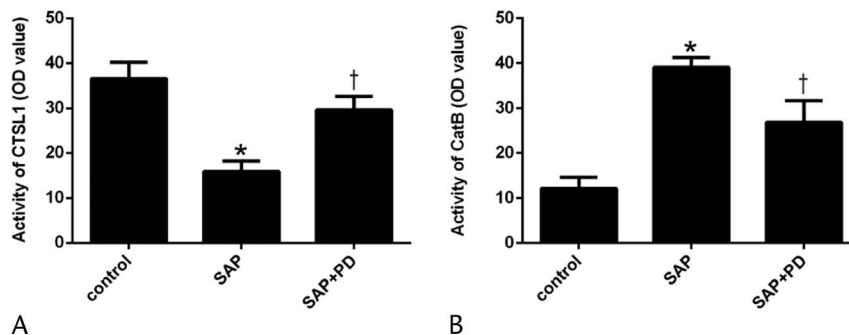


FIGURE 8. Detection of the activity of CTSL1 (A) and catB (B) in pancreatic tissue *Compared with the control group, $P < 0.05$. †Compared with the TLC group, $P < 0.05$.

features of lysosomal dysfunction are defective processing/activation of cathepsins and reductions in LAMP1 and LAMP2 levels, which lead to autophagic dysfunction, the activation of trypsinogen and the vacuolation of acinar cells.¹⁵ LAMP2 is one of the key proteins in the regulation of autophagic pathway and is mainly responsible for regulating autolysosome formation that results from autophagosome-lysosome fusion. As shown in Supplementary Figure 9, <http://links.lww.com/MPA/A771>, lack of LAMP2 expression led to impaired autolysosome formation and massive autophagosome retention. Gukovsky et al showed that the lack of LAMP2 aggravated the severity of AP and induced the necrosis of pancreatic cells.² The present study found that LAMP2 expression was reduced in the TLC group but elevated in the PD + TLC group. This finding indicates that PD98059 pretreatment significantly enhanced the expression of LAMP2 in pancreatic tissues and promoted the formation of autolysosomes. It can be inferred that PD98059 restores the activity of the blocked downstream pathway of autophagy by upregulating the expression of LAMP2 and alleviating the impairment of autolysosome formation, thereby reducing the accumulation and aberrant activation of trypsinogen. Trypsinogen can be converted to active trypsin by cathepsin B (CTSB). Cathepsin L another member of the papain family of cysteine proteases, has enzymatic properties similar to those of CTSB. Cathepsin L exhibits stronger endoproteolytic activity than CTSB and is capable of degrading trypsinogen and trypsin. Therefore, CTSL may alleviate the deleterious effects of CTSB by reducing trypsin activity.¹⁶ The present study examined CTSL1 and found that the expression level and activity of CTSL1 were significantly increased in the group pretreated with PD98059 compared with the TLC group. This finding indirectly demonstrated that PD98059 reduces the amount of active trypsin in autolysosomes and improves the protein degradation efficiency of autophagic pathways by regulating the ratio and activity of CTSL in lysosomes and improving lysosomal function, thereby reducing the severity of pancreatitis.

The optimum pH for the enzymatic reactions in lysosomes is 5.0. At pH 7.0, lysosomal enzymes become inactivated. If the pH level far exceeds its optimal value, the activity of lysosomal acid hydrolases is reduced, and the degradation of autolysosomes is impaired. As a result, the downstream pathway of autophagy is blocked, and a large amount of autophagosomes accumulate. In the present study, it was found that lysosomal pH was significantly higher in the TLC group compared with the normal group. This finding indicates that the activity of lysosomal enzymes was reduced in the TLC group. In contrast, there was no significant difference in lysosomal pH between the group pretreated with PD98059 and the TLC group. Animal experiments showed that lysosomal pH was significantly downregulated in the SAP group after pretreatment with PD98059. The results of the in vitro and in vivo experiments suggest that PD98059 exerts a regulatory effect on lysosomal pH. Moreover, the regulatory effects of PD98059 on the expression levels and activities of acid hydrolases (such as CTSL) were particularly significant.

In clinical practice, the most commonly examined indicator of pancreatitis is serum α -amylase (AMS) and can be used as a diagnostic criterion for AP. The higher the AMS levels of the patient, the greater the level of attention should be given.¹⁷ Trypsinogen activation peptide is a degradation product of trypsinogen produced during trypsinogen activation. A recent study has shown that TAP can be used as an index for early prediction of AP severity. The higher the TAP concentration, the higher the degree of inflammation.¹⁸ In the mouse model of AP constructed by Letoha et al,¹⁹ pretreatment with the MAPK pathway inhibitor PD98059 significantly attenuated the destruction of acinar structure and reduced the infiltration of inflammatory cells into pancreatic tissues. In addition, compared with the AP group, the degree

of pathological necrosis was markedly reduced, and the AMS concentration was significantly decreased after PD98059 pretreatment. The results indicated that pancreatic injury was significantly improved after PD98059 pretreatment. The present study examined AMS and TAP in a rat model of SAP and found that AMS activity and TAP levels had declined from their peak values at 24 hours after the induction of AP. However, AMS activity and TAP levels remained significantly elevated in comparison to the control group ($P < 0.05$). After pretreatment with PD98059, AMS and TAP were significantly decreased in the SAP + PD group compared with the SAP group ($P < 0.05$). Pathological examination of the pancreas showed that the extent of pancreatic injury was significantly reduced in the SAP + PD group, and the change was statistically significant ($P < 0.05$). The results of pathological examination further demonstrated that PD98059 was able to reduce the severity of AP and improve the prognosis.

In summary, both the cell-based experiments and the animal experiments conducted in the present study demonstrated that PD98059 pretreatment significantly inhibited the activation of trypsinogen in pancreatic acinar cells and reduced pathological injury. In addition, PD98059 pretreatment downregulated the expression levels of Beclin 1 and LC3II, regulated autophagy, promoted the expression of LAMP and CTSL, and improved lysosomal function. The above results indicate that PD98059 releases the blockage of autophagic flux and alleviates lysosomal dysfunction in pancreatic acinar cells, thereby inhibiting the intracellular activation of trypsinogen. Thus, PD98059 has a protective effect on pancreatic tissues. However, the pathogenesis of AP is very complicated. Autophagy is also affected by many factors, and the specific mechanisms of action of autophagy remain unclear. Therefore, whether PD98059 can be used as a new target for AP treatment requires further investigation.

REFERENCES

- Gukovsky I, Pandol SJ, Gukovskaya AS. Organellar dysfunction in the pathogenesis of pancreatitis. *Antioxid Redox Signal*. 2011;15:2699–2710.
- Gukovsky I, Pandol SJ, Mareninova OA, et al. Impaired autophagy and organellar dysfunction in pancreatitis. *J Gastroenterol Hepatol*. 2012;27(suppl 2):27–32.
- Eriksson I, Joosten M, Roberg K, et al. The histone deacetylase inhibitor trichostatin A reduces lysosomal pH and enhances cisplatin-induced apoptosis. *Exp Cell Res*. 2013;319:12–20.
- Hashimoto D, Ohmuraya M, Hirota M, et al. Involvement of autophagy in trypsinogen activation within the pancreatic acinar cells. *J Cell Biol*. 2008;181:1065–1072.
- Ohmuraya M, Yamamura K. Autophagy and acute pancreatitis: a novel autophagy theory for trypsinogen activation. *Autophagy*. 2008;4:1060–1062.
- Zhou YY, Li Y, Jiang WQ, et al. MAPK/JNK signalling: a potential autophagy regulation pathway. *Biosci Rep*. 2015;35. pii: e00199.
- Martinez-Lopez N, Athonvarangkul D, Mishall P, et al. Autophagy proteins regulate ERK phosphorylation. *Nat Commun*. 2013;4:2799.
- Clemons AP, Holstein DM, Galli A, et al. Cerulein-induced acute pancreatitis in the rat is significantly ameliorated by treatment with MEK1/2 inhibitors U0126 and PD98059. *Pancreas*. 2002;25:251–259.
- Mareninova OA, Hermann K, French SW, et al. Impaired autophagic flux mediates acinar cell vacuole formation and trypsinogen activation in rodent models of acute pancreatitis. *J Clin Invest*. 2009;119:3340–3355.
- Tiedje C, Holtmann H, Gaestel M. The role of mammalian MAPK signaling in regulation of cytokine mRNA stability and translation. *J Interferon Cytokine Res*. 2014;34:220–232.

11. Zhou P, Tan YZ, Wang HJ, et al. Cytoprotective effect of autophagy on phagocytosis of apoptotic cells by macrophages. *Exp Cell Res*. 2016;348:165–176.
12. Gukovskaya AS, Gukovsky I. Autophagy and pancreatitis. *Am J Physiol Gastrointest Liver Physiol*. 2012;303:G993–G1003.
13. Gukovsky I, Gukovskaya AS. Impaired autophagy underlies key pathological responses of acute pancreatitis. *Autophagy*. 2010;6:428–429.
14. Yamaguchi H, Kimura T, Mimura K, et al. Activation of proteases in cerulein-induced pancreatitis. *Pancreas*. 1989;4:565–571.
15. Boland B, Kumar A, Lee S, et al. Autophagy induction and autophagosome clearance in neurons: relationship to autophagic pathology in Alzheimer's disease. *J Neurosci*. 2008;28:6926–6937.
16. Wartmann T, Mayerle J, Kähne T, et al. Cathepsin L inactivates human trypsinogen, whereas cathepsin L-deletion reduces the severity of pancreatitis in mice. *Gastroenterology*. 2010;138:726–737.
17. Wang Q, Wang H, Yang X, et al. A sensitive one-step method for quantitative detection of α -amylase in serum and urine using a personal glucose meter. *Analyst*. 2015;140:1161–1165.
18. Staubli SM, Oertli D, Nebiker CA. Laboratory markers predicting severity of acute pancreatitis. *Crit Rev Clin Lab Sci*. 2015;52:273–283.
19. Letoha T, Fehér LZ, Pecze L, et al. Therapeutic proteasome inhibition in experimental acute pancreatitis. *World J Gastroenterol*. 2007;13:4452–4457.